

YEMEN FLOOD SUSCEPTIBILITY ANALYSIS METHODOLOGY

INTRODUCTION

Flooding has inflicted devastating consequences upon Yemen in the past. Unfortunately, due to climate change, flood events are predicted to increase in frequency, magnitude and seasonality globally [1]. Floods cause loss of life and property damage, consequences which are more impacting on vulnerable communities like those affected by the Yemeni crisis. Floods are among the most frequent and costly natural disasters in terms of human and economic loss [2]. Mitigating the effect of natural disasters is becoming ever more relevant in the Yemen humanitarian crisis intervention due to the looming climate crisis.

This country-wide analysis aims to provide humanitarian actors with an improved understanding of the exposure of vulnerable populations to flooding in Yemen. Though this analysis does not represent comprehensive hydrological predictions, it can serve as a means to inform humanitarian programming with relation to flood risk and preparedness.

RATIONALE

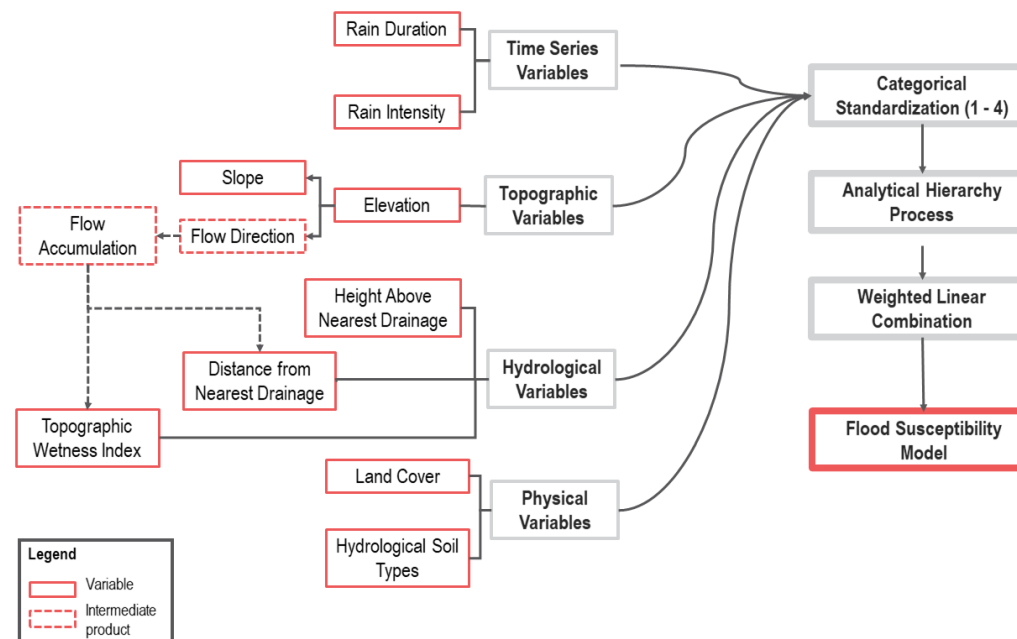
The objective of this analysis is to identify areas in Yemen that are the most and least susceptible to flooding. Though there are existing maps that show past flooding events in Yemen, there are none highlighting the susceptibility to future flooding at the level of detail of this analysis (60 and 30 m resolution at country scale and up to 3 m resolution for specific areas at city scale), and which use the approach chosen for this analysis.

[UNEP GRID](#) and [ThinkHazard!](#) both have information on flood potential in Yemen. The UNEP GRID Global Risk flood risk dataset indicates 25 -1000 year flood hazard areas but doesn't readily disclose the modelling methods. The ThinkHazard! dataset has a Yemen specific profile but the findings are generalized to the district-level.

The REACH Yemen Flood Susceptibility analysis is based on a methodology that does not need data collected on the field and builds upon free and open datasets*.

*For versions of the model at a detail below 10 m, proprietary satellite images are used to generate elevation and its derived products.

WORKFLOW



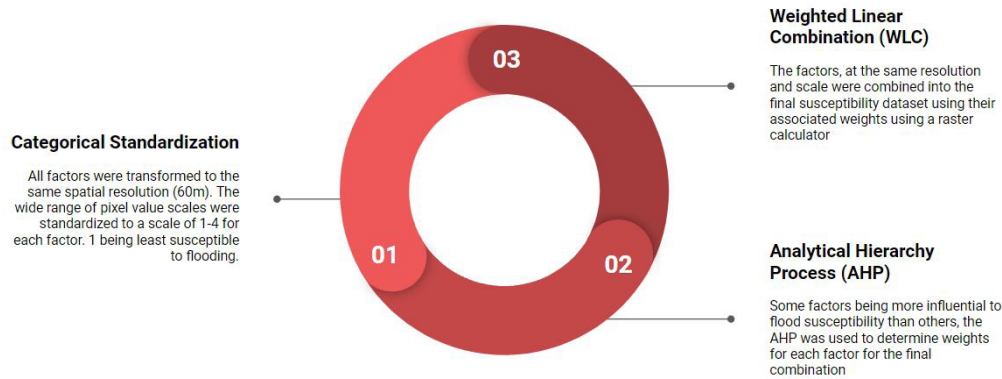
DATASETS

| Source | Variable(s) | Resolution | Period | Link |
|--|---|-------------------|-------------|---|
| Global Hydrologic Soil Groups v1 | Soil Type | ~250 m | 1900 - 2015 | https://daac.ornl.gov/SOILS/guides/Global_Hydrologic_Soil_Group.html |
| CHIRPS Daily: InfrarRed Precipitation w/ Station Data v2 | Rain Intensity, Rain Duration | ~0.05 arc degrees | 1984-2018 | https://developers.google.com/earth-engine/datasets/catalog/UCSB-CHG_CHIRPS_DAILY |
| MODIS Landcover | Landcover | 500 m | 2016 | https://developers.google.com/earth-engine/datasets/catalog/MODIS_006_MCD12Q1 |
| NASADEM HGT v001 | Elevation, Slope, Topographic Wetness Index, Distance from Nearest Drainage | ~30 m | - | https://pdaac.usgs.gov/products/nasadem_hgtv001/ |
| Height Above Nearest Drainage | Height above Nearest Drainage | 90 m | - | https://code.earthengine.google.com/f7174cd11d23d78baca4021f2645ef33 |

METHODOLOGY

The mapping of flood susceptible areas involves the analysis of multiple criteria that collectively contribute to the likelihood of floods. Using geographical location as a commonality between datasets, GIS platforms enable the combination of contributing flood factors into one single dataset representing susceptibility in every point of the analysed region. This method leverages modelling capabilities of Google Earth Engine and ArcGIS Pro to assess the biophysical vulnerability of the region based on a variety of satellite imagery and spatial datasets.

Nine influencing parameters are the input factors of the model. These describe different characteristics of the region, such as topographical, physical and hydrological properties. The construction of the model itself can be summarized in three steps:



CATEGORICAL STANDARDIZATION

All input datasets have varying scales and units of measurement. In order to calculate susceptibility as a cumulative score of all factors, they were each standardized to the same scale. The pixel values were reclassified into the same categorical scale from one to four - one being least susceptible and four being most susceptible to flooding. This was done using the quartile classification method for the continuous datasets, so that each class contains the same number of values and all classes are equally represented. For Land Cover, classes were ranked based the degree of imperviousness, intended as the capacity of the ground to be impenetrable to water [24]. Soil was classified according to its infiltration capacity, the lower the infiltration the higher the rank.

FACTORS USED

- Elevation
- Slope
- Topographic Wetness Index (TWI)
- Rainfall Intensity (Ave. Max. Annual)
- Rainfall Duration (Ave. Max. Annual)
- Distance from Nearest Drainage (DND)
- Height Above Nearest Drainage (HAND)
- Land-cover
- Soil Type

ANALYTICAL HIERARCHY PROCESS

Multi-criteria analysis using AHP facilitates multi-source data combinations which is a real advantage in improving the reliability of the susceptibility analysis. "AHP uses hierarchical structures to represent a problem and, then, develop priorities for alternatives based on the judgment of the user based on paired comparisons. Evaluation criteria and their weights must be determined according to their importance" [1]. For each factor, the degree of influence on flood risk was assigned depending on the importance of its effect. The pairwise comparison chart was used to obtain the weights based on their rating. In order to build the pairwise comparison chart, 12 studies were compared, applying the AHP technique for floods in arid and semiarid regions (see Pairwise Comparison and AHP References section). For each pair of factors, the relative weight was plotted on a graph and a linear regression equation was calculated. These equations were used to define the relative weights of each element of the chart. This approach was used so that the hierarchy and relative magnitude of final weights matches that of literature.

Pairwise Comparison Chart

| | Land-cover | Soil Type | Elevation | Slope | TWI | Rain (Int. + Dur) | DND | HAND | Final Weight |
|------------------|------------|-----------|-----------|-------|------|-------------------|------|-------|--------------|
| Land-cover | 1 | 6.63 | 2.41 | 0.49 | 0.92 | 5.97 | 0.08 | 0.39 | 0.100 |
| Soil Type | 0.15 | 1 | 0.16 | 0.28 | 2.28 | 3.50 | 0.19 | 0.12 | 0.063 |
| Elevation | 0.41 | 6.07 | 1 | 2.09 | 0.24 | 0.64 | 3.44 | 0.13 | 0.099 |
| Slope | 2.04 | 3.63 | 0.48 | 1 | 0.19 | 0.65 | 0.64 | 16.86 | 0.156 |
| TWI | 1.08 | 0.44 | 4.16 | 5.38 | 1 | 0.87 | 5.03 | 0.44 | 0.168 |
| Rain (Int.+Dur.) | 0.17 | 0.29 | 1.56 | 1.54 | 1.15 | 1 | 0.58 | 0.09 | 0.058 |
| DND | 12.48 | 5.34 | 0.29 | 1.56 | 0.20 | 1.71 | 1 | 1.42 | 0.148 |
| HAND | 2.58 | 8.57 | 7.57 | 0.06 | 2.25 | 11.55 | 0.70 | 1 | 0.208 |

WEIGHTED LINEAR COMBINATION

The weighted linear combination (WLC) was adopted to produce the final flood susceptibility map. This method used the ArcGIS Raster Calculator tool to aggregate all the weighted factor rasters to produce the final output.

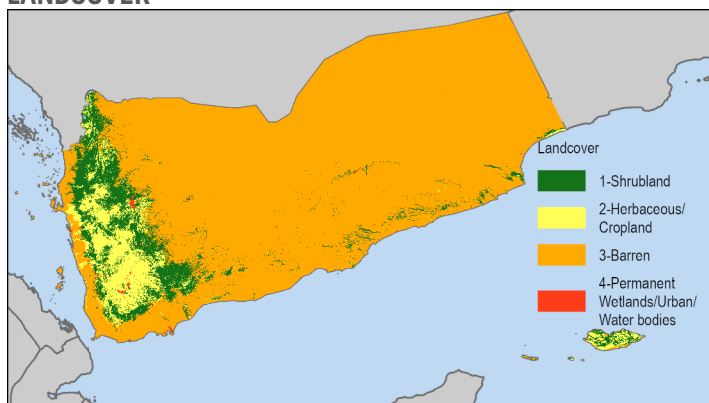
$$\text{Flood Susceptibility} = (\text{Land cover} * 0.100) + (\text{Soil} * 0.063) + (\text{Elevation} * 0.099) + (\text{Slope} * 0.156) + (\text{TWI} * 0.168) + ((\text{Rain Intensity} + \text{Rain Duration}) * 0.058) + (\text{DND} * 0.148) + (\text{HAND} * 0.208)$$

Due to technical limitations, the end product of this analysis is a map representing flood susceptibility rather than risk. Risk implies consequential basis of analysis, and can be defined as demarcating "the areas under potential consequences where consequences can be those affecting human life, having economic effects or causing environmental changes for instance" [2]. With such definition, the final result of this analysis, which depends on natural factors (rather than social or economic ones), will be indicative of flood susceptibility rather than risk.

DATA PROCESSING & ANALYSIS

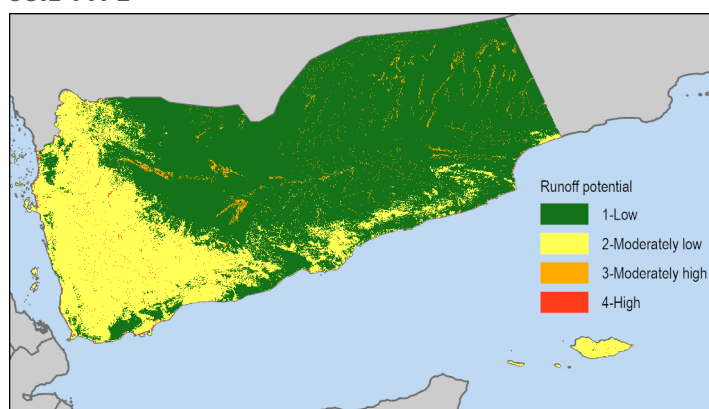
Nine criteria were considered in this susceptibility analysis. Their datasets were either readily available for download online, or derived through spatial analysis from existing datasets, and satellite images. The data processing was done mostly in Google Earth Engine (GEE) and on ArcGIS Pro. Following the processing of all of the datasets individually, they were combined using the Weighted Linear Combination (WLC) technique in ArcGIS Pro. The reasoning and processing of each factor is detailed here.

LANDCOVER



This factor is important when considering runoff, as the composition of the landscape, whether natural or man-made, affects infiltration [15].

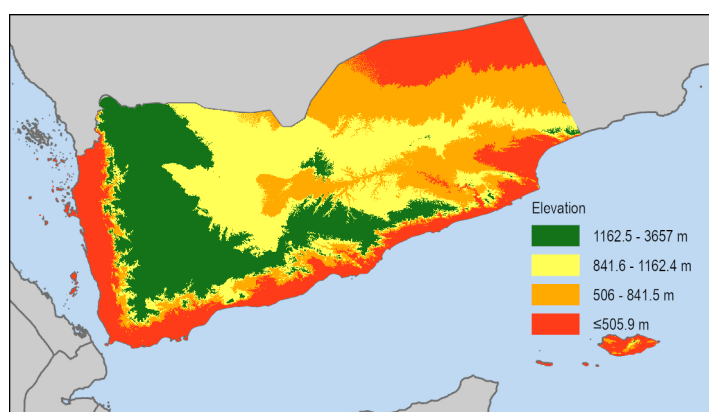
SOIL TYPE



Soil texture and its degree of wetness (directly related to the depth of the groundwater table), deeply affect the runoff potential, and therefore the magnitude of inundation resulting from intense rainfall [25].

For this reason, the Global Hydrologic Soil Groups (HYSOGs250m) was used. Within this dataset, soil is classified based on its permeability and infiltration properties.

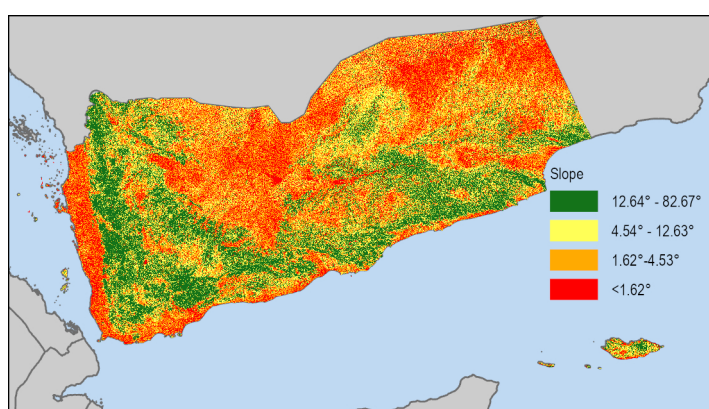
ELEVATION



Floods are typically identified in low elevations because rainfall on higher elevations accumulates downhill due to gravitational forces towards lower elevations.

The dataset used is the NASADEM at 30m resolution, while Digital Terrain Models (DTMs) were extracted from very high resolution satellite images to obtain a spatial resolution below 10m.

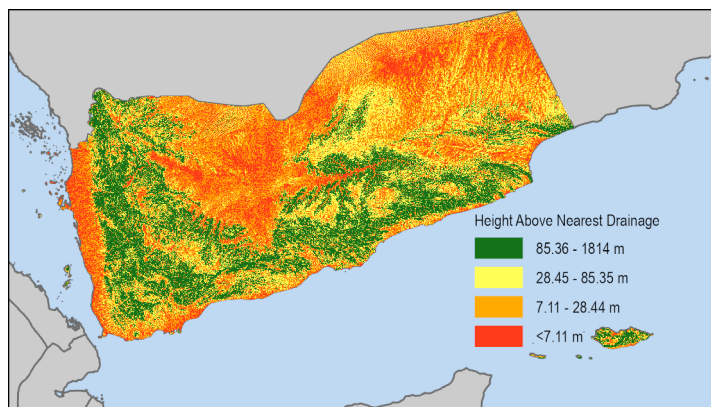
SLOPE



Floods caused by extraordinary rainfall events are the result of accumulated runoff. Steep slopes are less likely to be inundated during intense rainfall because the water drains down-slope, where flooding is more likely to occur [3].

This factor was calculated from the DEM using the homonymous ArcGIS Pro tool. It is measured in degrees.

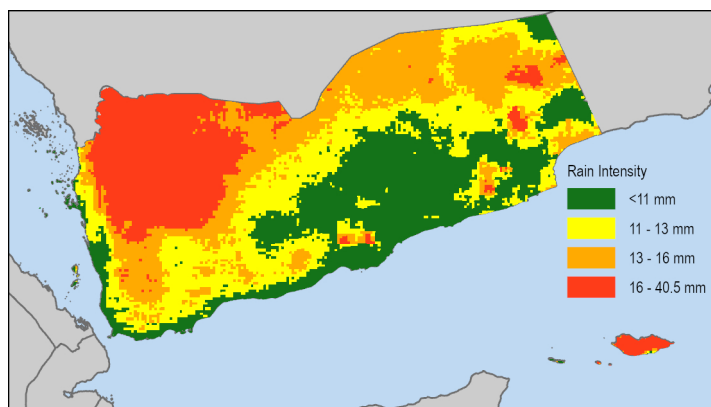
HEIGHT ABOVE NEAREST DRAINAGE (HAND)



This is a proxy for hydrological drainage networks, incorporating topography and gravitational potentials in a manner that normalizes terrain heights. It captures local topographic heterogeneities, fundamental for flood hazard mapping [29].

This data was downloaded from GEE. [Code*](#)

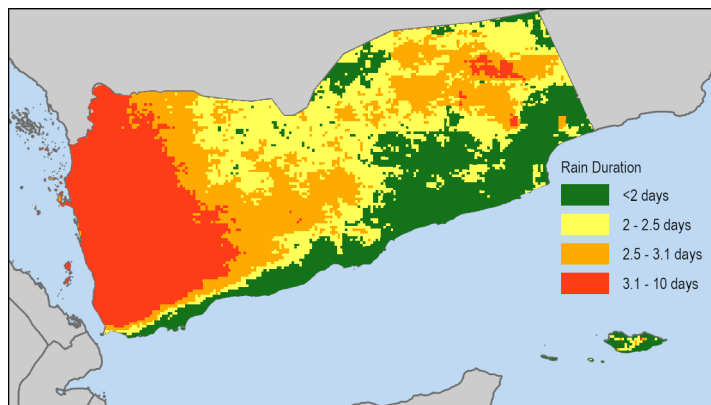
RAINFALL INTENSITY



Floods are often caused by intense rainfall events. Areas experiencing the highest amounts of rainfall are more susceptible to flooding.

Daily rainfall data available on GEE was analysed within the GEE cloud computing platform to derive the average of maximum annual rainfall per year from 1984 to 2018. [Code*](#)

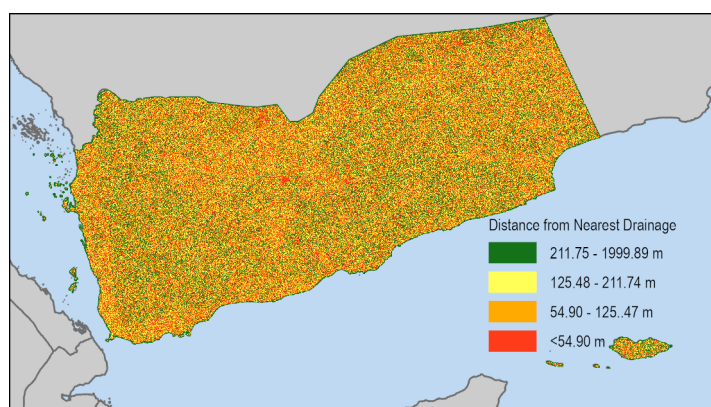
RAINFALL DURATION



Floods are often caused by intense rainfall events. Areas experiencing long periods of rainfall are more susceptible to flooding

Daily rainfall data available on GEE was analysed within the GEE cloud computing platform to derive an average of the longest period of consecutive days of rainfall per year from 1984 to 2017. [Code*](#)

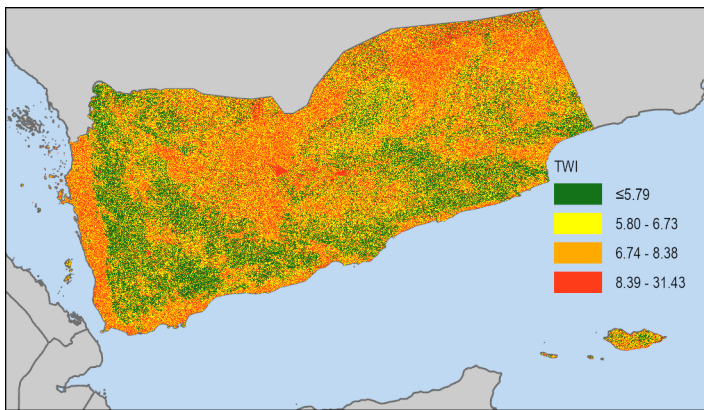
DISTANCE FROM NEAREST DRAINAGE



Main drainage channels, where flow accumulates are relatively more likely to flood [15]. Overflow from drainage areas is the reason proximity is an important consideration.

It is the result of the following geo-processing steps, carried out on ArcGIS Pro: a river network mask was generated from the flow accumulation dataset, with a threshold of 100. Through the Euclidean Distance tool, the Distance from Nearest Drainage was calculated from such a network, with 2000 m maximum distance limit for the calculation.

TOPOGRAPHIC WETNESS INDEX (TWI)



This dataset is the result of the following equation, calculated on ArcGIS Pro:

$$\begin{cases} \ln\left(\frac{\text{flowAcc} + 1}{\tan(\text{slope}_{rad})}\right) \text{pixelsize} & \text{Slope} > 0 \\ \ln\left(\frac{\text{flowAcc} + 1}{\tan\left(\pi \frac{0.00565}{180}\right)}\right) \text{pixelsize} & \text{Slope} = 0 \end{cases}$$

Where *flowAcc* is flow accumulation, *slope_{rad}* is the slope in radians. The value 0.00565 was used as an approximation of a flat slope.

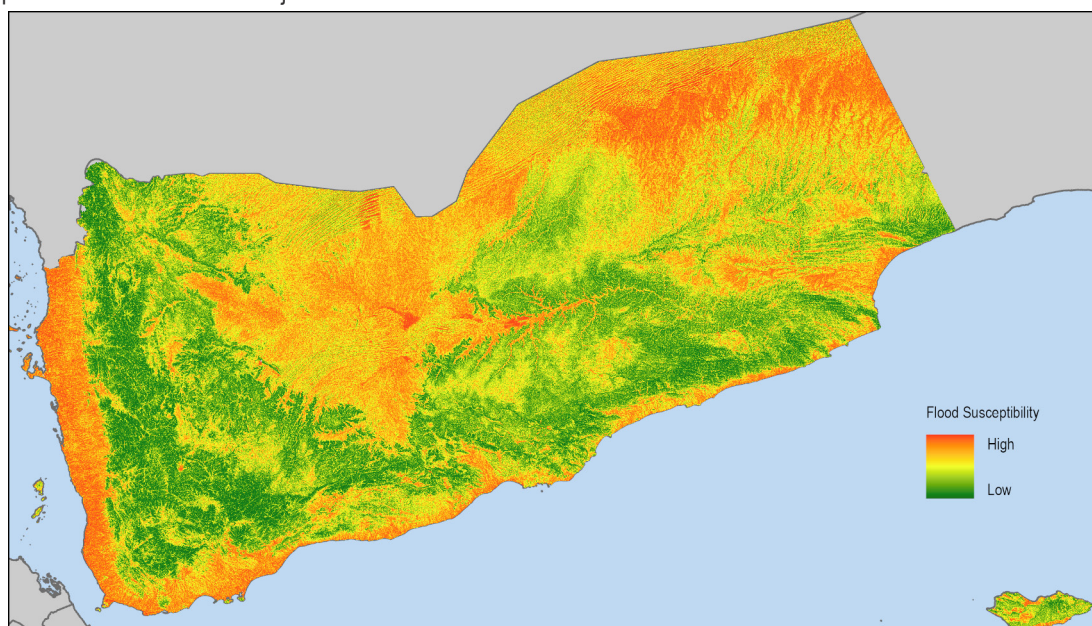
*Note: you can only access code links if you have a Google Earth Engine account

RESULT

The final result of the calculations is an image where each pixel has continuous values ranging from 1 to 4 as a representation of the susceptibility to flooding in each location. The output is significantly impacted by the weights, however, the compounding values retain information about the degree of relative susceptibility.

Two types of map products have been published based on this methodology: a flood susceptibility map at 30m resolution, and 2 case studies at a larger scale, specifically over the cities of Lahj and Ma'rib, at 3 and 8 m resolution respectively. This has allowed to have better understanding of where flooding is most likely to occur at the city level and which neighborhoods are more exposed than others.

In addition, as a complementary product of Lahj and Ma'rib flood susceptibility maps is the Flood Water Level Maps. These represent areas which might flood if the river water level rises of 1, 2, 3 and 4 meters respectively. They are based on a Digital Terrain Model (DTM) generated by very high resolution satellite images in stereo mode. This technique only keeps into account the topography of the area without considering factors such as rainfall, soil types or runoff. It is however useful for understanding where flooding can occur due to the overflow of the river, especially near villages and settlements. The final product has the spatial resolution of 3m for Lahj and 8 m for Ma'rib.



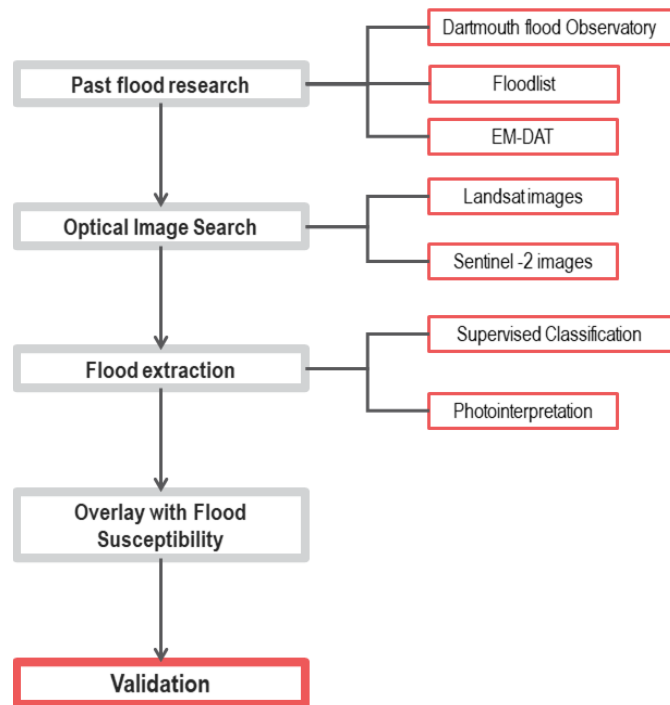
TWI is a runoff model that exploits slope, elevation, flow accumulation and flow direction to determine the capability of a land surface to accumulate water [4].

Flow accumulation is the calculated from Flow direction, which is extracted from a hydrologically conditioned (or depression less) DEM. All these parameters were calculated using the following tools in ArcGIS Pro: Fill, Flow direction and Flow accumulation tools from the Spatial Analyst Toolbox.

ACCURACY ASSESSMENT

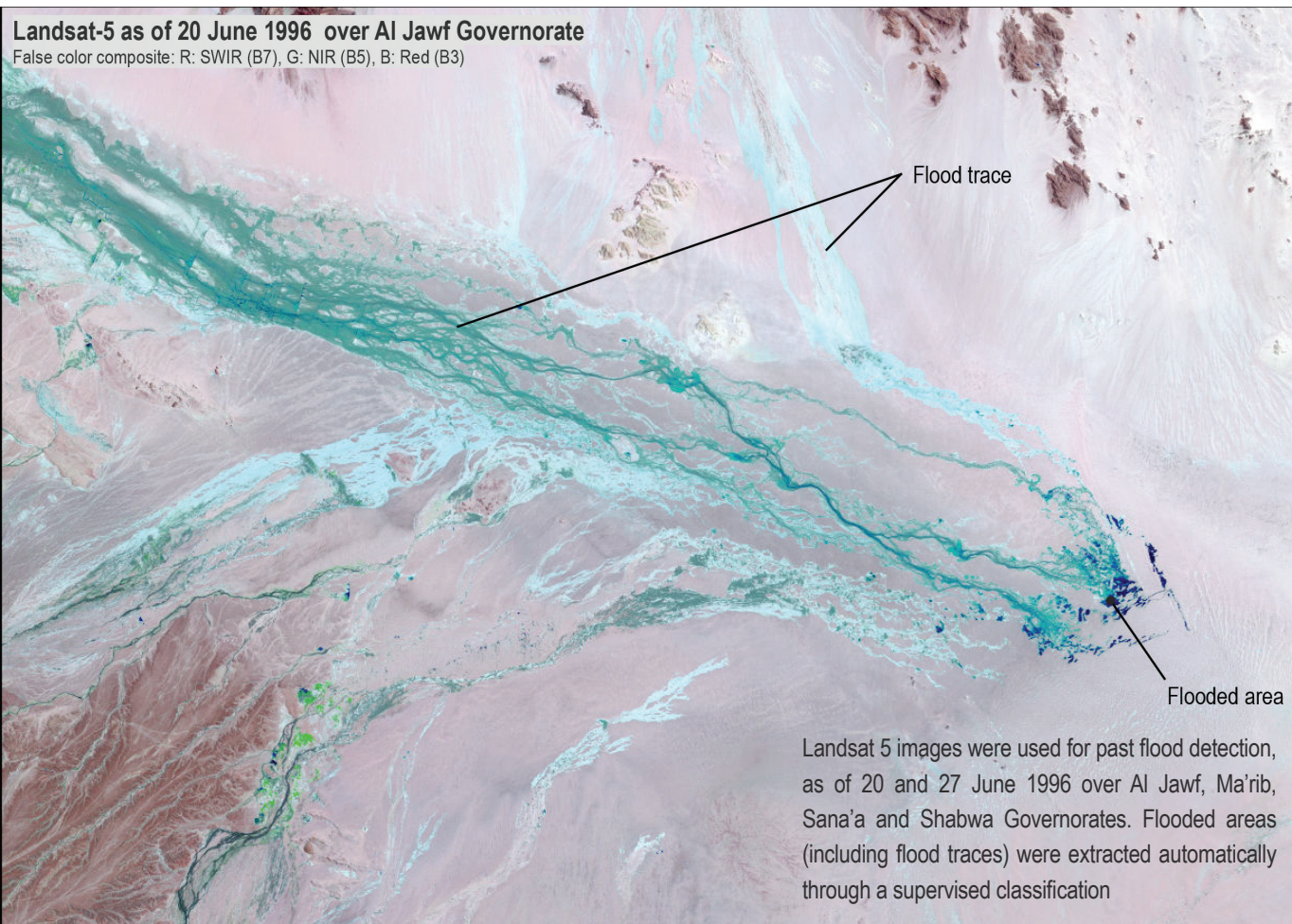
An accuracy assessment was conducted by comparing previously flooded areas with the model. Two events were chosen, based on the availability of optical satellite data and on the extent of the event: June 1996 and June 2019.

WORKFLOW

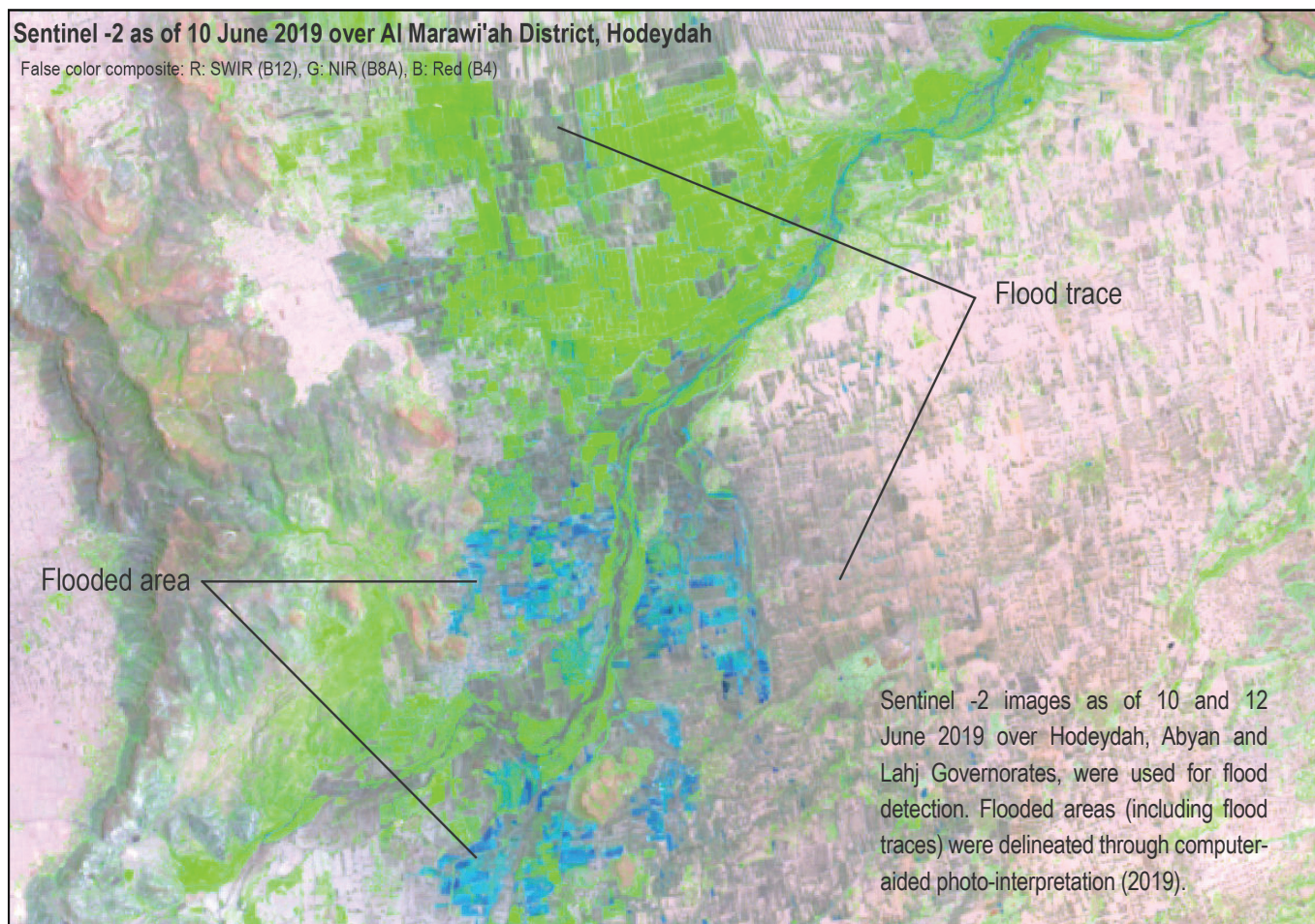


HISTORICAL FLOOD SEARCH

In 1996 the tropical Cyclone 02A made landfall in Oman and Yemen between June 11 and 12 1996. In Yemen, the storm produced the heaviest rainfall in 70 years, reaching 189 mm in Ma'rib. The floods damaged or destroyed 1,068 km of roads and 21 bridges. The storm also washed away 42,800 ha of crop fields, accounting for US \$100 million in damage. At least 1,820 houses were destroyed. Overall damage was estimated at US \$1.2 billion, and there were 338 deaths.



Strong winds, heavy rain and flash floods hit several parts of Yemen from 08 June, 2019, causing major damages and at least 3 deaths. The most affected governorate was Aden, which witnessed 77 mm of rain almost all in 3 hours. Houses and roads were washed away and submerged, while in rural areas wadis transformed to rivers, due to the runoff from hillsides.



FLOOD EXTRACTION

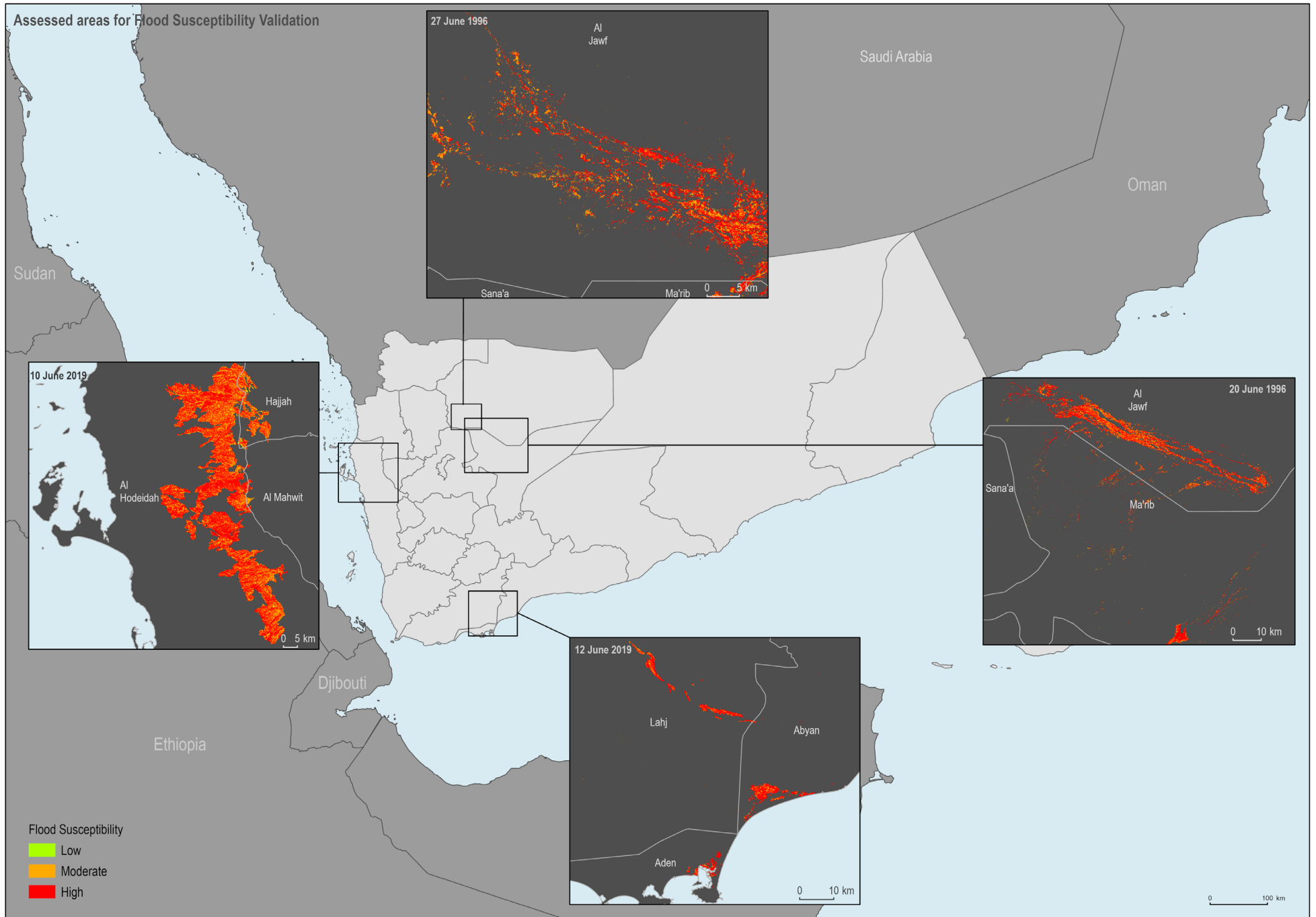
The validation was made by overlaying the flooded areas with the flood susceptibility model and verifying the susceptibility value for each point in the flood mask.

To do so, the model's values were categorized into three classes: low susceptibility (values between 1 and 2), moderate susceptibility (values between 2 and 3) and high susceptibility (value between 3 and 4).

The tables below show the extent and percentage of flooded area the model assigns to each class. In general, over 60% of the flooded areas are recognized by the model as high susceptibility (Abyan and Lahj in June 2019 with 80% have the highest accuracy, while June 2019 Hodeydah 63.5% has the lowest accuracy), and more than 99% of the flooded areas are represented as moderate to high susceptibility.

| Timeline | 20 June 1996 | | 27 June 1996 | |
|--------------|-------------------------|------------|-------------------------|------------|
| Governorates | Al Jawf, Ma'rib, Sana'a | | Al Jawf, Ma'rib | |
| Class | Area (Km ²) | Percentage | Area (Km ²) | Percentage |
| Low | 0.601 | 0.18% | 0.104 | 0.08% |
| Moderate | 102.524 | 31.09% | 47.945 | 34.57% |
| High | 226.624 | 68.73% | 90.644 | 65.36% |
| Total | 329.749 | | 138.694 | |

| Timeline | 10 June 2019 | | 12 June 2019 | |
|--------------|--------------------------------|------------|-------------------------|------------|
| Governorates | Al Hodeidah, Hajjah, Al Mahwit | | Lahj, Aden, Abyan | |
| Class | Area (Km ²) | Percentage | Area (Km ²) | Percentage |
| Low | 4.046 | 0.30% | 0.050 | 0.06% |
| Moderate | 480.874 | 36.20% | 17.161 | 19.66% |
| High | 843.512 | 63.50% | 70.060 | 80.28% |
| Total | 1328.432 | | 87.271 | |



NOTICE

This interpretation of flood susceptibility is not predictive, and does not portray flood risk. Instead, the analysis indicated areas more or less susceptible to flooding based on physical land features and rainfall.

The analysis highlights areas which are highly susceptible to flood in the case of an intense rainfall event. Detailed risk assessment is necessary prior to detailed flood prevention planning.

Recommended areas of improvement for future work relating to this exploratory research:

- Inclusion of variables accounting for economic and social variables, allowing for the assessment of risk rather than susceptibility
- Collaborating with hydrological experts to determine unique and precise fuzzy membership transformation methods for factors rather than quantile distribution for all
- Improve upon the used method of literature review by consulting with hydrological experts on the ranking of factors in the analytical hierarchy process
- Improve the Land Cover dataset so as to obtain one with a finer resolution. The possibility of leveraging optical satellite imagery with supervised classification techniques should be explored.

Note that this is an exploratory analysis and the results are not to be used in strategic planning. The methods and results aren't verified by hydrological experts. The data, designations and boundaries contained in these images are not warranted to be error-free and do not imply acceptance by the REACH partners, associated, donors referenced.

ABOUT REACH

REACH is a joint initiative that facilitates the development of information tools and products that enhance the capacity of aid actors to make evidence-based decisions in emergency, recovery and development contexts. By doing so, REACH contributes to ensuring that communities affected by emergencies receive the support they need. All REACH activities are conducted in support to and within the framework of inter-agency aid coordination mechanisms. For more information, please visit our website at www.reach-initiative.org, contact us directly at yemen@reach-initiative.org or follow us on Twitter at [@REACH_info](https://twitter.com/REACH_info).

Download static flood susceptibility maps by governorate at the [REACH Resource Centre](#)

RESOURCES

METHODOLOGICAL REFERENCES

1. Danumah, J.H., Odai, S.N., Saley, B.M. et al. Flood risk assessment and mapping in Abidjan district using multi-criteria analysis (AHP) model and geoinformation techniques, (cote d'ivoire). *Geoenvirom Disasters* 3, 10 (2016). <https://doi.org/10.1186/s40677-016-0044-y>
2. Pradhan, Biswajeet. (2009). Flood susceptible mapping and risk area delineation using logistic regression, GIS and remote sensing. *Journal of Spatial Hydrology*. 9. 1-18.
3. Yun Chen, Rui Liu, Damian Barrett, Lei Gao, Mingwei Zhou, Luigi Renzullo, Irina Emelyanova, A spatial assessment framework for evaluating flood risk under extreme climates, *Science of The Total Environment*, Volume 538, 2015, Pages 512-523,
4. De Risi, R., Jalayer, F., De Paola, F. et al. Delineation of flooding risk hotspots based on digital elevation model, calculated and historical flooding extents: the case of Ouagadougou. *Stoch Environ Res Risk Assess* 32, 1545–1559 (2018). <https://doi.org/10.1007/s00477-017-1450-8>
5. Giustarini, L.; Chini, M.; Hostache, R.; Pappenberger, F.; Matgen, P. Flood Hazard Mapping Combining Hydrodynamic Modeling and Multi Annual Remote Sensing data. *Remote Sens.* 2015, 7, 14200-14226.
6. Dahri, Noura & Ellouze, Manel & Abdelfattah, Atoui & Abida, Habib. (2016). Mapping flood risk areas IN GABES BASIN (SOUTH-EASTERN TUNISIA).
7. Zhaoli Wang, Chengguang Lai, Xiaohong Chen, Bing Yang, Shiwei Zhao, Xiaoyan Bai, Flood hazard risk assessment model based on random forest, *Journal of Hydrology*, Volume 527, 2015, Pages 1130-1141,ISSN 0022-1694,
8. Elsheikh, R.F.A. & Ouerghi, Sarra & Elhag, Abdel. (2015). Flood Risk Map Based on GIS, and Multi Criteria Techniques (Case Study Terengganu Malaysia). *Journal of Geographic Information System*. 07. 348-357. 10.4236/jgis.2015.74027.
9. Doyle, C.S., Sullivan, J.A., Mahtta, R., & Pandey, B. (2017). Assessing biophysical and social vulnerability to natural hazards in Uttarakhand, India.
10. Dieu Tien Bui, Biswajeet Pradhan, Haleh Nampak, Quang-Thanh Bui, Quynh-An Tran, Quoc-Phi Nguyen,Hybrid artificial intelligence approach based on neural fuzzy inference model and metaheuristic optimization for flood susceptibility modeling in a high-frequency tropical cyclone area using GIS, *Journal of Hydrology*, Volume 540, 2016, Pages 317-33

PAIRWISE COMPARISON AND AHP REFERENCES

11. Vahid Nourani and Soghra Andaryani, Flood Susceptibility Mapping in Densely Populated Urban Areas Using Mcdm and Fuzzy Techniques, EasyChair Preprint no. 2244, 2019
12. Ismail Elkhrachy, Flash Flood Hazard Mapping Using Satellite Images and GIS Tools: A case study of Najran City, Kingdom of Saudi Arabia (KSA), The Egyptian Journal of Remote Sensing and Space Science, Volume 18, Issue 2, 2015, Pages 261-278.
13. Khaleghi, Somaiyeh & Mahmoodi, Mehran. (2017). Assessment of flood hazard zonation in a mountainous area based on gis and analytical hierarchy process. 12. 311-322.
14. Hammami, Salma & Zouhri, Lahcen & Souissi, Dhekra & Souei, Ali & Zghibi, Adel & Marzougui, Amira & Dlala, Mahmoud. (2019). Application of the GIS based multi-criteria decision analysis and analytical hierarchy process (AHP) in the flood susceptibility mapping (Tunisia). Arabian Journal of Geosciences. 12. 10.1007/s12517-019-4754-9.
15. Omid Rahmati, Hossein Zeinivand & Mosa Besharat (2016) Flood hazard zoning in Yasooj region, Iran, using GIS and multi-criteria decision analysis, Geomatics, Natural Hazards and Risk, 7:3, 1000-1017, DOI: 10.1080/19475705.2015.1045043
16. Talha, S. & Maanan, Mohamed & Atika, H. & Rhinane, Hassan. (2019). PREDICTION OF FLASH FLOOD SUSCEPTIBILITY USING FUZZY ANALYTICAL HIERARCHY PROCESS (FAHP) ALGORITHMS AND GIS: A STUDY CASE OF GUELMIM REGION IN SOUTHWESTERN OF MOROCCO. ISPRS - International Archives of the Photogrammetry, Remote Sensing and Spatial Information Sciences. XLII-4/W19. 407-414. 10.5194/isprs-archives-XLII-4-W19-407-2019.
17. Mahmoud, Mohammed & Li, Xuxiang. (2019). Low-Cost Solution for Assessment of Urban Flash Flood Impacts Using Sentinel-2 Satellite Images and Fuzzy Analytic Hierarchy Process: A Case Study of Ras Ghareb City, Egypt. Advances in Civil Engineering. 2019. 1-15. 10.1155/2019/2561215.
18. Almodayan, A. (2018) Analytical Hierarchy (AHP) Process Method for Environmental Hazard Mapping for Jeddah City, Saudi Arabia. Journal of Geoscience and Environment Protection, 6, 143-159. <https://doi.org/10.4236/gep.2018.66011>
19. Lappas I., Kallioras A., Flood Susceptibility Assessment through GIS-Based Multi-Criteria Approach and Analytical Hierarchy Process (AHP) in a River Basin in Central Greece, International Research Journal of Engineering and Technology (IRJET), 6, 3, 2019, pp. 738-751.
20. Shereif H. Mahmoud, Thian Yew Gan, Multi-criteria approach to develop flood susceptibility maps in arid regions of Middle East, Journal of Cleaner Production, Volume 196, 2018, Pages 216-229.
21. Dahri, N., Abida, H. Monte Carlo simulation-aided analytical hierarchy process (AHP) for flood susceptibility mapping in Gabes Basin (southeastern Tunisia). Environ Earth Sci 76, 302 (2017). <https://doi.org/10.1007/s12665-017-6619-4>
22. Dhekra Souissi, Lahcen Zouhri, Salma Hammami, Mohamed Haythem, Msaddek, Adel Zghibi & Mahmoud Dlala (2019): GIS-based MCDM - AHP modeling for flood susceptibility mapping of arid areas, southeastern Tunisia, Geocarto International

23. Ahmed M. Youssef, Mahmoud A. Hegab, 10 - Flood-Hazard Assessment Modeling Using Multicriteria Analysis and GIS: A Case Study—Ras Gharib Area, Egypt, Editor(s): Hamid Reza Pourghasemi, Candan Gokceoglu, Spatial Modeling in GIS and R for Earth and Environmental Sciences, Elsevier, 2019, Pages 229-257
24. Hodgson, Michael & Jensen, John & Tullis, Jason & Riordan, Kevin & Archer, Clark. (2003). Synergistic Use of Lidar and Color Aerial Photography for Mapping Urban Parcel Imperviousness. Photogrammetric Engineering & Remote Sensing. 69. 973-980. 10.14358/PERS.69.9.973.

INPUT DATASETS REFERENCES

25. Ross, C.W., L. Prihodko, J. Anchang, S. Kumar, W. Ji, and N.P. Hanan. 2018. Global Hydrologic Soil Groups (HYSOGs250m) for Curve Number-Based Runoff Modeling. ORNL DAAC, Oak Ridge, Tennessee, USA. <https://doi.org/10.3334/ORNLDAAC/1566>
26. Funk, Chris, Pete Peterson, Martin Landsfeld, Diego Pedreros, James Verdin, Shraddhanand Shukla, Gregory Husak, James Rowland, Laura Harrison, Andrew Hoell & Joel Michaelsen. "The climate hazards infrared precipitation with stations—a new environmental record for monitoring extremes". Scientific Data 2, 150066. doi:10.1038/sdata.2015.66 2015.
27. Friedl, M., Sulla-Menashe, D. (2019). MCD12Q1 MODIS/Terra+Aqua Land Cover Type Yearly L3 Global 500m SIN Grid V006 [Data set]. NASA EOSDIS Land Processes DAAC. Accessed 2020-03-24 from <https://doi.org/10.5067/MODIS/MCD12Q1.006>
28. NASA JPL (2020). NASADEM Merged DEM Global 1 arc second V001 [Data set]. NASA EOSDIS Land Processes DAAC. https://doi.org/10.5067/MEaSURES/NASADEM/NASADEM_HGT.001
29. Donchyts, Gennadiy & Winsemius, Hessel & Schellekens, Jaap & Erickson, Tyler & Gao, Hongkai & Savenije, Hubert & van de Giesen, Nick. (2016). Global 30m Height Above the Nearest Drainage. 10.13140/RG.2.1.3956.8880.

ACCURACY ASSESSMENT REFERENCES

30. <http://floodlist.com/>
31. <https://www.emdat.be/>
32. <http://floodobservatory.colorado.edu/>

DONORS

